Mislocalization of CFTR expression in acute pancreatitis and the beneficial effect of VX-661 + VX-770 treatment on disease severity

Gabriella Fűr[1], Emese Réka Bálint[1], Erik Márk Orján[1], Zsolt Balla[1,8], Eszter Sára Kormányos[1], Beáta Czira[1], Attila Szűcs[1], Dénes Péter Kovács[1], Petra Pallagi[2,3], József Maléth[2,3], Viktória Venglovecz[4], Péter Hegyi[5,6,7], Lóránd Kiss[1], Zoltán Rakonczay Jr.[1*]*

[1] Department of Pathophysiology, University of Szeged, Szeged, Hungary

[2] First Department of Medicine, University of Szeged, Szeged, Hungary.

[3] Momentum Epithelial Cell Signalling and Secretion Research Group, Hungarian Academy of Sciences-University of Szeged, Szeged, Hungary.

[4] Department of Pharmacology and Pharmacotherapy, University of Szeged, Szeged, Hungary

[5] Institute for Translational Medicine and First Department of Medicine, University of Pécs, Pécs, Hungary.

[6] Momentum Translational Gastroenterology Research Group, Hungarian Academy of Sciences-University of Szeged, Szeged, Hungary.

[7] Szentágothai Research Centre, University of Pécs, Pécs, Hungary.

[8] Current address: Institute of Applied Sciences, Department of Environmental Biology and Education, Juhász Gyula Faculty of Education, University of Szeged, Szeged, Hungary.

[*] Lóránd Kiss and Zoltán Rakonczay Jr. have contributed equally to this work.

Corresponding authors:

Zoltán Rakonczay Jr. MD, PhD, DSc and Lóránd Kiss, PhD

Department of Pathophysiology, University of Szeged.

Mailing address: Semmelweis u. 1., H-6725 Szeged, Hungary

E-mail: rakonczay.zoltan@med.u-szeged.hu and lorand.kiss.work@gmail.com

Telephone number: +36-62-545-994

This is an Accepted Article that has been peer-reviewed and approved for publication in The Journal of Physiology, but has yet to undergo copy-editing and proof correction. Please cite this article as an 'Accepted Article'; doi: 10.1113/JP281765.

Key points summary

- Cystic fibrosis transmembrane conductance regulator (CFTR) is an important ion channel in epithelial cells. Its malfunction has several serious consequences, like developing or aggravating acute pancreatitis (AP).
- Here, we investigated the localization and expression of CFTR during cerulein-induced AP in mice and determined the effects of CFTR corrector (VX-661) and potentiator (VX-770) on disease severity.
- CFTR mRNA expression was significantly increased, and mislocalization of CFTR protein was observed in AP compared to the control group.
- Interestingly, pre-treatment of AP mice with VX-661 + VX-770 significantly reduced the extent of pancreatic tissue damage by 20-30%.
- *In vitro* administration of VX-661 + VX-770 significantly increased the fluid secretion of ducts derived from AP animals.
- Based on our results, the utilization of CFTR correctors and potentiators should be further investigated in AP.

Abstract

Cystic fibrosis transmembrane conductance regulator (CFTR) has essential role in maintaining pancreatic ductal function. Impaired CFTR function can trigger acute pancreatitis (AP) and exacerbate disease severity. We aimed to investigate the localization and expression of CFTR during AP, and determined the effects of CFTR corrector (VX-661) and potentiator (VX-770) on disease severity.

AP was induced in FVB/n mice by 6-10 hourly intraperitoneal injections of 50µg/kg cerulein. Some mice were pre-treated with 5-6 daily injections of 2mg/kg VX-661+VX-770. Control animals were administered physiological saline instead of cerulein and DMSO instead of VX compounds. AP severity was determined by measuring laboratory and histological parameters; CFTR and CK19 expressions were measured. Activity of ion transporters was followed by intracellular pH or fluid secretion measurement of isolated pancreatic intra-/interlobular ducts.

Cerulein-induced AP severity was greatest between 12-24h. CFTR mRNA expression was significantly increased 24h after AP induction. Immunohistochemistry demonstrated disturbed staining morphology of CFTR and CK19 proteins in AP. Mislocalization of CFTR protein was observed from 6h, while expression increased at 24h compared to control. Ductal HCO_3^- transport activity was significantly increased 6h after AP induction. AP mice pre-treatment with VX-661+VX-770 significantly reduced the extent of tissue damage by about 20-30%, but other parameters were unchanged. Interestingly, VX-661+VX-770 *in vitro* administration significantly increased the fluid secretion of ducts derived from AP animals. This study described the course of the CFTR expression and mislocalization in cerulein-induced AP. Our results suggest that the beneficial effects of CFTR correctors and potentiators should be further investigated in AP.

Introduction

The exocrine pancreas mainly consists of acinar and ductal cells (Czakó et al., 2009). Ductal cells provide structural framework for pancreas, convey digestive enzymes secreted by acini, neutralize the acidic fluid of the acini as well as the gastric juice entering into the duodenum (Pallagi et al., 2015). Ductal cells produce 2.5 litre of alkaline secretion daily which may contain up to 140 mM HCO_3^- (Hegyi & Rakonczay, 2015). Several transporters and different mechanisms are involved in fluid and HCO_3^- secretion. Basolateral transporters like Na^+/HCO_3^- cotransporter (NBC), Na^+/H^+ exchanger (NHE) or H^+-ATPase contribute to HCO_3^- uptake into ductal cells. In addition, CO_2 diffuses into the cells from the blood and carbonic anhydrases convert it to HCO_3^-. Apical ion transporters which participate in HCO_3^- secretion are solute carrier family 26 A3 and A6 (SLC26A3, SLC26A6), cystic fibrosis transmembrane conductance regulator (CFTR), and Anoctamin-1 (ANO1). Among these ion transporters, CFTR is the most prominent due to its numerous roles in secretion and regulation (Hegyi et al., 2016; Kim et al., 2020). In fact, CFTR is present in these epithelial cells as a signalling hub. Its most important functions include Cl^- or HCO_3^- secretion, and regulation of ion channels like SLC26A6 (Rakonczay et al., 2008). CFTR is mainly stimulated by cyclic AMP; however, intracellular Ca^{2+} concentration also influences its activity. CFTR alters Ca^{2+} signalling through direct connection with sarco/endoplasmic reticulum Ca^{2+}-ATPase (SERCA) and plasma membrane Ca^{2+}-ATPase (PMCA) channels (Philippe et al., 2015) or by functional coupling with transient receptor potential canonical 6 (Antigny et al., 2008). Moreover, the presence of CFTR is necessary for proper function of mitochondria (Madácsy et al., 2018).

Acute pancreatitis (AP) is the sudden inflammation of the pancreas and one of the most common gastrointestinal diseases (Peery et al., 2015). Its incidence shows increasing tendency, and it is more than 30 per 100 000 population in Europe (Roberts et al., 2013 and 2017). The two main causes of AP are excessive alcohol consumption and gallstone diseases (Forsmark et al., 2016; Párniczky et al., 2016). The pathomechanism of AP is complex and not fully revealed. The underlying mechanisms of AP involve toxic intracellular Ca^{2+} overload inducing premature activation of digestive enzymes, NF-κB activation, impaired autophagy, mitochondrial dysfunctions, and impairment of ductal function (Barreto et al., 2021). The therapy of AP is only supportive and there is no specific drug against it (Crockett et al., 2018).

Pancreatic ductal cell damage also occurs during AP due to disease-inducing factors (such as ethanol and bile acids) and intraductal enzyme activation. Furthermore, these factors dose-dependently affect ductal function as well (Hegyi and Rakonczay, 2015). Low concentrations of ethanol and bile acids stimulate, while higher concentrations inhibit ductal functions (Judák et al., 2014; Maléth et al., 2011 and 2015; Venglovecz et al., 2008). Activated trypsin in ductal lumen inhibits CFTR via proteinase-activated receptor 2 (Pallagi et al., 2011). Moreover, the impaired ductal function due to CFTR mutations in cystic fibrosis (Ooi et al., 2011) or ductal obstructions (Li and Tian, 2017; Mujica et al., 2000) can lead to chronic pancreatitis or AP, respectively. CFTR inhibition in AP and the consequent disease aggravation by ductal impairment cause a vicious cycle.

Recently, several drugs were clinically approved to improve CFTR expression, localization and function by correcting protein folding or to potentiate its activity in cystic fibrosis (Amaral, 2021). Among them the CFTR corrector lumacaftor (VX-809), tezacaftor (VX-661), elexacaftor (VX-445) and the CFTR potentiator, ivacaftor (VX-770) were the most effective. CFTR activity markedly contributes to proper ductal function. The disturbance or reduction of ductal function is one of the key factors in initiation of AP.

In the past two decades, the earlier mentioned studies mainly utilized healthy ducts to reveal how different etiological factors of AP (ethanol, bile acids, unsaturated fatty acids, etc.) affect pancreatic ductal epithelial functions. Therefore, the complex effects of AP were not investigated on ducts. Our first aim was to reveal changes in pancreatic ductal function and CFTR expression during the course of AP. Then our second aim was to test whether the correction and potentiation of CFTR affect the disease severity.

Materials and methods

Animals

8-10 week-old male FVB/n mice were used for experiments. The animals were obtained from Charles River Laboratories Inc. (Wilmington, MA, USA) and housed in the departmental animal facility in a constant room temperature of 24 °C with a 12 h light-dark cycle and were allowed *ad libitum* to water and standard laboratory chow (Biofarm, Zagyvaszántó, Hungary). Animal experiments were performed in compliance with the European Union Directive 2010/63/EU and the Hungarian Government Decree 40/2013 (II.14.). Experiments were approved by both local (University of Szeged) and national ethics committees (X./3355/2017) for investigations involving animals. In our study, all animals were sacrificed via intraperitoneal (i.p.) injection of 200 mg/kg pentobarbital (Bimeda MTC, Cambridge, Canada).

Materials

All chemicals were obtained from Merck/Sigma-Aldrich Kft. (Budapest, Hungary) unless indicated otherwise. Cerulein (Cer) was acquired from Glentham Life Sciences (Corsham, United Kingdom); VX-661 (tezacaftor) and VX-770 (ivacaftor) were obtained from Cayman Chemical (Ann Arbor, MI, USA); amylase activity kit was procured from Diagnosticum (Budapest, Hungary); anti-CFTR antibody was purchased from Alomone Labs (Jerusalem, Israel); AlexaFluor488 goat anti-rabbit secondary antibody and Hoechst 33342 were from ThermoFisher Scientific (Waltham, MA, USA); anti-Cytokeratin-19 antibody was obtained from Abcam (Cambridge; United Kingdom); RNA/cDNA kits: DreamTaq DNA Polymerase, DreamTaq™ Green Buffer, dNTP mix 25 mM, GeneRuler 100 bp DNA Ladder, TRIzol™ Plus RNA Purification Kit, UltraPure™ Ethidium Bromide, GeneRuler™ 1 kb Plus DNA Ladder, High-Capacity cDNA Reverse Transcription Kit and Luminaris Color HiGreen qPCR Master Mix were obtained from ThermoFisher Scientific; 2.7-bis-(2-carboxyethyl)-5-(and-6-) carboxyfluorescein-acetoxymethylester (BCECF-AM) was purchased from Biotium (Fremont, CA, USA).

Cer, VX-661 and VX-770 were dissolved in DMSO and Cer was further diluted in physiological saline (PS) before injection. The solutions used for ductal (intracellular pH, pH_i, and fluid secretion) measurements and immunohistochemistry are presented in Table 1.

	Standard HEPES (mM)	Standard HCO_3^-/CO_2 (mM)	NH_4^+ in HCO_3^-/CO_2 (mM)	Tris-buffered saline (mM)
NaCl	140	115	95	150
KCl	5	5	5	-
$MgCl_2$	1	1	1	-
$CaCl_2$	1	1	1	-
HEPES	10	-	-	-
Glucose	10	10	10	-
$NaHCO_3$		25	25	-
NH_4Cl			20	-
Trizma base				50
pH	7.4	set by 5 % CO_2 and 95 % O_2 bubbling	set by 5 % CO_2 and 95 % O_2 bubbling	7.4

In vivo experiments: acute pancreatitis induction and treatment with VX-661 + VX-770

Two different experimental setups were utilized in this work (Fig. 1). In the first part of the study, AP was evoked to reveal its effect on CFTR expression and ductal function (Fig. 1*A*). In the second part of our work, CFTR corrector and potentiator (VX-661 and VX-770, respectively), administration was combined with AP induction (Fig. 1*B*). Necrotizing AP was induced by hourly i.p. injection of 6 or 10 × 50 µg/kg Cer (5 µg/ml) in FVB/n mice as described previously (Pallagi et al., 2014). VX-661 and VX-770 were administered i.p. at 2 mg/kg once a day before and during AP. The doses of VX-661 and VX-770 were chosen based on the study by Zeng et al. (2017). Control groups were given PS solution instead of CER, and DMSO instead of VX compounds. Animals were sacrificed at 0, 6, 12, 24, 48, and 72 h when the effect of AP on ducts and CFTR were investigated. In case of VX-661 + VX-770 combination, the first termination time was at 24 h and the second at 48 h.

Immediately after opening the abdomen, a small piece of pancreas was removed for measurement of mRNA expression. Then blood was collected through cardiac puncture (~400µl) and placed on ice until serum separation. After that, the remaining part of the pancreas was rapidly excised and was cleaned from fat and lymph nodes on ice, then cut into pieces. A small piece of the pancreatic tissue was fixed in 8% neutral formaldehyde solution for histological analysis, the rest was immediately frozen in liquid nitrogen and stored at −80 °C until biochemical assay. For dry-wet mass measurements, a small sample was stored in an Eppendorf tube. For immunohistochemical staining procedures, a small piece of the pancreas was frozen in cryomatrix at –80 °C. Blood samples were centrifuged at 2500 g for 15 min at 4 °C and the sera were stored at –20 °C until amylase activity measurement.

Laboratory measurements

Pancreatic myeloperoxidase (MPO) activity is a hallmark of leukocytic infiltration and was measured according to Kuebler et al. (1996). MPO activities were normalized to total protein content as measured by the Lowry method (Lowry et al., 1959). To evaluate pancreatic water content, the wet weight (WW) of the pancreata was measured, then the tissues were dried for 48 h at 100 °C and the dry weight (DW) was also measured. The tissue water content was calculated as: [(WW-DW)/WW]×100. Serum amylase activity was measured on a Fluorostar Optima plate reader from BMG Labtech (Ortenberg, Germany) with a colorimetric kinetic method using a commercial amylase activity kit. Absorbance of the samples was detected at 405 nm.

Histological examination

Formalin-fixed and paraffin embedded pancreatic tissues were sectioned to 3 µm. These sections were stained with hematoxylin and eosin and were scored by independent experts blinded to the experimental protocol, then the scores related to the same samples were averaged. To quantify cellular damage, leukocyte infiltration and oedema grades a semiquantitative scoring system was used according to Kui et. al (2015). Briefly, edema was scored from 0-3 points (0: none; 1: patchy interlobular; 2: diffuse interlobular; 3: diffuse interlobular and intra-acinar), leukocyte infiltration from 0-4 points (0: none; 1: patchy interlobular; 2: moderate diffuse interlobular; 3: mild diffuse interlobular; 4: diffuse interlobular and intra-acinar). Percentage of cellular damage was also evaluated. In addition, the extent of vacuolization was determined (0: none; 1: diffuse/mild; 2: diffuse/moderate; 3: diffuse/severe).

mRNA extraction and reverse transcription

A small piece of pancreas was placed on ice in 1 ml TRIzol reagent in a 13 ml centrifuge tube and was homogenised immediately with IKA Ultra Turrax (Type: TP18/10). Then the tissue

homogenate was instantly placed on liquid nitrogen and stored at –80 °C until use (for max. of 1 or 2 days). Total RNA purification was performed in three steps. In the first step, phase separation was performed by adding 200 µl of chloroform to the samples and shaking vigorously for 15 min, allowing to stand, and then centrifuging at 12000 g for 15 min at 4 °C. From the resulting 3 phases, the top aqueous phase was aspirated into an empty Eppendorf tube and 500 µl of isopropanol was added. This was vortexed and then allowed to stand for a few min and after that it was centrifuged at 12000 g for 10 min at 4 °C. RNA precipitated in the Eppendorf tubes. The supernatant was removed and 1 mL of 75% alcohol was added. It was vortexed and centrifuged at 7500 g for 5 min at 4 °C. After removal of the supernatant, the excess ethanol was evaporated briefly and then the RNA was redissolved in 70 µl of RNAse-free water. RNA was stored at –80 °C until further use.

RNA concentration was measured using a NanoDrop instrument from ThermoFisher Scientific (Waltham, MA, USA). We considered the optimal ranges for RNA: A260/A280: 1.9-2.1 and A260-A230: 1.8-2.5. RNA integrity was examined after agarose gel electrophoresis.

2 µg of total RNA was used for reverse transcription. PCR protocol for the reverse transcription was started at 25 °C for 10 min, followed by 37 °C for 2 h, 85 °C for 5 min, then 4 °C. cDNA was stored at –20 °C until further use.

Quantitative real-time PCR

The total reaction mix volume was 10 µl. The components of the reaction mixture were the following: 1.67 µl cDNA sample, 0.4 mM forward and reverse primer, Luminaris Color HiGreen qPCR Master Mix and nuclease-free water. The protocol for the quantitative real-time PCR was started at 50 °C for 2 min, then 95 °C for 10 min, followed by 40 cycles of amplification: 95 °C for 15 sec, 60 °C or 64 °C for 30 sec (depending on the primers), 72 °C for 30 sec then a Melt Curve from 70 °C to 95 °C for 5 sec with 0.5 °C increment. Our primers used in relative gene expression measurements (Table 2.) were checked with the Oligoanalyzer program from Integrated DNA Technologies (Iowa, USA; https://www.idtdna.com/pages/tools/oligoanalyzer). Gradient PCR was and performed to determine the appropriate annealing temperature of the primers. The *Slc26a3* and *Slc26a6* primer pairs have been used previously in our laboratory (Molnár et al., 2020). The housekeeping gene in mRNA studies was *Rplp0*.

Gene	5'-3' Primer pairs	Product (bp)
Cftr	F: GACGAGCCAAAAGCATTGAC	157
	R: TGGTCCAGCTGAAGAAGAGT	
Slc26a3	F: CTCGGACCCCAATGCTTCTT	127
	R: CCCCAGGAGCAACTGAATGA	
Slc26a6	F: GAGCTGTTTGCAACGCTTGT	121
	R: CCTGGTTACTGTCCACACGG	
Ck19	F: ATCGTCTCGCCTCCTACTT	250
	R: TCTGTCTCAAACTTGGTTCTG	
Rplp0	F: AGATTCGGGATATGCTGTTGGC	109
	R: TCGGGTCCTAGACCAGTGTTC	

Table 2. Oligonucleotide primer pairs used for determination of relative gene expression.

Immunohistochemistry

The cryomatrix-embedded pancreatic tissues derived from animals were sliced by a Leica Cryostat at 7 µm thickness. Sections were fixed in 2 % paraformaldehyde for 20 min. Washing periods were administered with Tris-buffered saline (TBS) solution (pH 7.4). Antigen retrieval was performed with 0.1 % Triton X-100 in TBS solution for 10 min. Blocking was performed for 1 h with 5 % bovine serum albumin-TBS solution. These sections were then incubated with anti-CFTR rabbit polyclonal antibody (dilution 1:400) overnight at 4 °C. The following day the samples were incubated with AlexaFluor 488 goat anti-rabbit secondary antibody (dilution 1:500) for 1 h in the dark at room temperature. After a few washing steps, co-immunostaining was performed with the AlexaFluor647-conjugated CK19 antibody (dilution 1:100, CK19 is a ductal marker protein). Nuclei were counterstained with Hoechst 33342 (dilution 1:400). Tissue slices were mounted with Fluoromount and then analysed using a Zeiss LSM 880 confocal laser scanning microscope (Carl Zeiss Technika Kft., Budapest, Hungary). To quantify pancreatic ductal CFTR and CK19 expression, three or four representative large tile scan images were taken from each group by with the Zeiss LSM 880

microscope (in average 1500 x 1000 µm). Image J software was used to convert images to grey scale (16 bit), and threshold function was used to select the positively stained area based on the fluorescence intensities. The area without tissue were excluded from the calculation.

Fluid secretion and intracellular pH measurement in cultured pancreatic ducts

Intra-/interlobular pancreatic ducts were isolated from control and AP mice after collagenase digestion by microdissection as described previously (Argent et al., 1986). In case of fluid secretion measurements, ducts were cultured for 6-14 h (which allowed sealing of their open ends) at 37 °C in a humidified atmosphere containing 5% CO_2. Some ducts were treated with 3 µM VX-661 and 1 µM VX-770 during incubation, while others subjected to the vehicle (0.5% DMSO) or only the medium.

Fluid secretion into the closed luminal space of the cultured pancreatic ducts was analysed using a swelling method (Fernandez-Salazar et al., 2004; Pallagi et al., 2014). Thenducts were transferred to a perfusion chamber and were attached to a coverslip pre-coated with 0.05 mg/ml poly-L-lysine. The ducts were perfused with different solutions in the following order: 1) standard HEPES, 2) standard HEPES with 5 µM forskolin 3) standard HCO_3^-/CO_2 with 5 µM forskolin. Bright-field images were acquired at 1-min intervals using a Zeiss Axio Observer 7 with CMOS camera (Orca Flash4.0LT, Hamamatsu Photonics, Hamamatsu City, Japan). The integrity of the duct wall was checked at the end of each experiment by perfusing the chamber with a hypotonic solution (standard HEPES-buffered solution diluted 1:1 with distilled water). Digital images of the ducts were analysed using ImageJ software (National Institutes of Health, Bethesda, MD, USA) to obtain values for the area corresponding to the luminal space in each image.

pH_i measurements were started immediately after isolation and were carried out within 8 h thereafter using IX71 live cell imaging fluorescence microscope and Cell^R imaging system from Olympus (Budapest, Hungary). Alkali load method was applied to measure pancreatic ductal HCO_3^- secretion (Venglovecz et al., 2008). The HCO_3^- secretion was estimated by the rate of pH_i recovery from alkalization. The isolated ducts were loaded with pH sensitive BCECF-AM fluorescent dye (2 µM) for 20-30 min in standard HEPES solution at 37 °C in a humidified atmosphere containing 5 % CO_2. After that, ducts were perfused with solutions in the following order: 1) standard HEPES, 2) standard HCO_3^-/CO_2, 3) NH_4Cl in HCO_3^-/CO_2, 4) standard HCO_3^-/CO_2, 5) standard HEPES. Exposing ducts to 20 mM NH_4Cl caused alkalization of pH_i. The perfusion rate was 4-6 ml/min. Four to ten small areas (region of interests, ROIs) of 5-10 cells in each intact duct were monitored. The ducts were excited with light at wavelengths of 490 and 440 nm, and the 490/440 fluorescence emission ratio was measured at 535 nm. One pH_i measurement was obtained per second. The extent of pH_i change ($\Delta pH/\Delta t$) was calculated by linear regression analysis.

Statistical analysis

Graphs were generated by GraphPad Prism 9.2.0 (GraphPad Software, San Diego, CA, USA). Data are presented as means ± SDExperiments were evaluated by one- or two-way ANOVA followed by the Tukey HSD post hoc test (SPSS, IBM, Armonk, NY, USA). $P<0.05$ was accepted as statistically significant.

Results

The course of cerulein-induced acute pancreatitis severity

The progression of Cer-induced AP was followed from 0 to 72 h. Representative histological images show pancreatic tissues of mice sacrificed at different time points (Fig. 2*A*). Cer injection caused the greatest degree of cell damage at 24 h (Fig. 2*A-B*). This is adequately supported by the scoring results of vacuolization (Fig. 2*C*). Cell damage and vacuolization were significantly decreased at 48 and 72 h compared to 24 h groups (cell damage: $P = 0.0493$, $P < 0.0001$ respectively; vacuolization: $P = 0.0152$, $P = 0.0004$ respectively). Leukocyte infiltration was increased at 6, 12, 24, and 72 h after the first Cer injection compared to control (Fig. 2*D*; $P = 0.0002$, $P < 0.0001$, $P < 0.0001$, $P = 0.0582$, $P = 0.0165$ respectively). Changes in pancreatic MPO activity closely followed leukocyte infiltration and showed marked increases at 12 and 24 h (Fig. 2*E*). AP evoked significant elevations in pancreatic water content and serum amylase activity at 12 and 24 h compared to the control (0h) group (Fig. 2*F-G*; water content: $P = 0.0069$, $P = 0.0038$; serum amylase activity: $P < 0.0001$, $P = 0.0009$). Serum amylase activity was highest at 12 h, which then decreased back to control levels after 48 h (Fig. 2*G*). At 48-72 h, almost all histological and laboratory parameters showed decreased tendency compared to the 12 or 24 h groups.

Changes in CFTR expression and staining morphology during acute pancreatitis

Fig. 3 shows the mRNA expressions and protein staining during the time course of AP. The relative gene expression of *Cftr* mRNA was markedly increased during AP from 24 h compared to the control (Fig. 3*A, P = 0.0016*). The peak was detected at 48 h and almost 20-fold increase was measured in *Cftr* mRNA amount compared to the heathy group ($P < 0.0001$). This tendency was also observed in case of the ductal marker *Ck19* (Fig. 3*B*), but its mRNA had less marked increased expression than *Cftr*. *Ck19* mRNA expression was highest at 12 and 24 h after the initiation of AP. *Slc26a3* mRNA expression was also increased at 24 h, while the mRNA of *Slc26a6* was decreased between 24 and 72 h (Fig. 3*C-D*).

The percentage of area staining of CFTR and CK19 proteins was determined by fluorescent immunostainings. Fig. 3*E* shows representative images which was used to calculation of area staining. Six percent of pancreatic tissue in untreated group stained for CFTR (Fig. 3*F*). At the beginning of AP (6 and 12 h), the CFTR staining area showed decrease in tendency, but at 24 h the protein expression significantly increased compared to the control ($P = 0.0402$) or 6-12 h ($P = 0.0118$, $P = 0.0001$, respectively) treatment groups. The increase of CFTR protein expression is in accordance with the results of the mRNA measurements. CK19 staining area in the control group was approximately 20 % (Fig. 3*G*). This area of CK19 decreased in pancreatic tissue at the beginning of AP (6 h), while later on CK19 expression did not differ from the control group.

Detailed ductal structures were also captured after CFTR and CK19 immunostaining (Fig. 4). The physiological location of CFTR is in the apical membrane of the pancreatic ducts. Clearly, detectable ductal morphology was observed in the control animals in cases of both CFTR and CK19. The lumens of the stained intralobular ducts were approximately 2-3 μm in diameter, which could be followed through several μm. The nuclei were located close to the ductal lumen. Bigger interlobular ducts did not stainfor CFTR. Notably, AP even from 6 h disturbed the characteristic structure of the ductal tree. CFTR was mislocalized and both CFTR and CK19 proteins showed diffuse and perinuclear appearance. At 72 h after the initiation of the disease, some duct like structures appeared in stained tissue slices (Fig. 4, yellow arrow). CK19 and CFTR showed similar staining morphologies at all time points.

Pancreatic ductal HCO_3^- secretion during the course of acute pancreatitis

Alkali load method and measurement of pH_i changes during the cellular regeneration phase provided estimation of the HCO_3^- secretory function of isolated pancreatic ducts. This is mainly carried out by apical transporters (CFTR, SLC26A3, SLC26A6). When cellular alkalosis was stopped by ammonium elimination, the cells shortly became acidotic. The cellular regeneration from acidosis can activate basolateral transporters (eg. NBC, NHE or H^+-ATPase). Therefore, the regeneration rate from acidosis refers to the activity of basolateral transporters. At the early phase (6 h) of AP, HCO_3^- secretion by apical transporters was significantly increased as demonstrated by regeneration from alkali load (Fig. 5*A*; 0h vs. 6h: $P = 0.0071$). Basolateral transporter activity was also elevated when regeneration from acidosis was measured (Fig. 5*B*; 0h vs. 6h: $P = 0.0402$). However, from 12 to 72 h, the response to alkalosis and acidosis were not significantly different *vs*. the control group.

The combination of CFTR corrector VX-661 and CFTR potentiator VX-770 decreased the severity of AP

The combination of VX-661 and VX-770 by itself did not induce any gross adverse effects. In fact, the morphology of the pancreas was normal after administration of VX-661+VX-770, and the histological and laboratory parameters were also similar to the non-treated group (data not shown). The effects of VX-661+VX-770 on AP are shown in Fig. 6. Representative histological sections showed that AP damaged the pancreatic tissue and VX-661+VX-770 combination could ameliorate this damage (Fig. 6*A*). Almost all measured parameters were increased in AP groups compared to the control group (Fig. 6*B-F*). VX-661+VX-770 pre-treatment significantly decreased AP severity based on the extent of cell damage (Fig. 6*B*, P = 0.0093). We could not observe any significant difference in vacuolization over time or treatment in the AP groups (Fig. 6*C*). Measurements of pancreatic leukocyte infiltration and MPO activity showed similar kinetics, with no significant difference in the AP groups (Fig. 6*D-E*). No change was observed in pancreatic water content when the AP group was compared with the AP+VX-661+VX-770 group (Fig. 6*F*). In case of serum amylase activity, no significant difference was measured between the control and treated groups (Fig 6*G*).

The effect of CFTR corrector VX-661 and CFTR potentiator VX-770 on ductal morphology and protein expression in acute pancreatitis

CFTR and CK19 co-immunostainings showed normal ductal structures at 24 and 48 h in control groups (Fig. 7). AP disturbed the staining morphology of CFTR and CK19 at both 24 and 48 h. VX-661+VX-770 pre-treatment could not restore or improve the damaged ductal structure as demonstrated by CFTR or CK19 staining (Fig. 8). CFTR protein expression was increased by AP (P = 0.0022) while CK19 expression (P= 0.7637) was unchanged (Fig. 8*B-C*). VX-661+VX-770 pre-treatment had no effect on AP-induced alterations of CFTR and CK protein expressions.

VX-661 and VX-770 enhance fluid secretion in isolated pancreatic ducts from mice with acute pancreatitis

To investigate if fluid secretion is influenced by the treatment with VX-661 and VX-770, isolated ducts (treated with or without 0.5 % DMSO/VX-661 and VX-770) from control and AP mice were used, and their swelling was followed (Fig. 9). The cAMP agonist forskolin treatment significantly enhanced the swelling of ducts from control animals, especially in HCO_3^-/CO_2 containing buffer. DMSO administration did not influence changes in relative ductal luminal volume. Therefore, the corresponding groups treated with or without DMSO

were combined (i.e. cerulein and cerulein + DMSO). Ducts isolated from cerulein-treated animals showed tendency towards increased swelling rates compared to the PS-treated control mice, but this did not reach statistical significance (Fig. 9). Interestingly, VX-661 and VX-770 treated ducts showed significantly increased fluid secretory rate compared to the non-VX treated ducts derived from AP animals (Fig. 9*B*, P = 0.0146).

Discussion

The pathomechanism of AP is complex and the underlying processes are not completely understood. However, the important role of ductal impairment and the CFTR ion channel function in the pathomechanism of the disease is already known (Barreto et al., 2021; Hegyi et al., 2015). Recently several drugs appeared commercially (eg. VX-661 or VX-770) or are in clinical phases to restore impaired CFTR ion channel activity or the protein expression in diseases caused by mutations (e.g. cystic fibrosis). In this study, we found mislocalization of ductal CFTR during AP in mice, so the combination of VX-661 and VX-770 was applied to improve the function of pancreatic ducts during AP. Furthermore, to our best knowledge, this is the first study which investigated the *ex vivo* ductal function on pancreatic ducts isolated during AP as well.

Pallagi et al. (2011) have shown that premature activation of trypsin in AP causes ductal CFTR inhibition through proteinase-activated receptor 2 and elevation of intracellular Ca^{2+} concentration. Our study demonstrates that not just functional inhibition, but also mislocalization of CFTR may cause the decrease of ductal function. Our results demonstrate that AP induces the loss of CFTR staining along the ductal lumen, and CFTR staining was observed in the perinuclear region. Presumably, the inflammation and cellular stress direct CFTR proteins into proteosomes for degradation (Ahner et al., 2013). Interestingly, the mRNA expression of *Cftr* was unchanged in the beginning of AP (6-12 h) and was increased from 24 h. The protein expression of CFTR followed the mRNA changes and increased after 24h. Similar measurements were performed in our earlier work (Maléth et al., 2015). Human pancreata derived from patients with alcoholic AP and chronic pancreatitis were compared to normal pancreas. Alcoholic AP decreased *CFTR* mRNA and protein expressions in human samples, while chronic pancreatitis caused marked increase in mRNA expression and in cytoplasmic localization of CFTR proteins. In a cell culture and guinea pig AP model, Maléth et al. (2015) also demonstrated that ethanol and its metabolites decrease *Cftr* mRNA and protein expressions. Furthermore, ethanol and palmitoleic acid induced AP also caused CFTR

mislocalization in guinea pig. Consequently, the results of the present study and our earlier investigation (Maléth et al., 2015) showed that two different animal models of AP cause CFTR mislocalization, suggesting that this adverse effect is independent of the disease aetiology.

The *ex vivo* HCO_3^- secretion of isolated ducts was increased at 6 h after AP initiation, whereas at later time points it was similar to that of the non-AP group. These isolated ducts were derived from interlobular space and had bigger lumens, approximately 20-130 µm. However, CFTR expression was not observed in these ducts, only smaller (2-3 µm luminal diameter) intercalated ducts were stained for CFTR, as it was also shown by Burghardt et al. (2003) and Marino et al. (1991) in human samples. However, Fernandez-Salazar et al. (2004), Pallagi et al. (2014) and this work demonstrated functional CFTR activity in interlobular ducts by fluid secretion measurement. Therefore, the CFTR ion channel expression in mouse pancreatic interlobular ducts is low in contrast with intercalated ducts. Based on our results, the measured increase in ductal HCO_3^- secretion at 6 h after AP initiation mainly relates to activation of transporters other than CFTR, e.g. SLC26A3, SLC26A6, ANO1, NBC, NHE or H^+-ATPase. Our previous publications presented that etiological factors like ethanol or its metabolites and bile acids concentration dependently stimulate or inhibit the function of ducts (Judák et al., 2014; Maléth et al., 2011 and 2015; Venglovecz et al., 2008). These investigations used ducts derived from guinea-pig, which have prominent CFTR ion channel expression in interlobular ducts and could be activated by CFTR agonists (e.g. cAMP; Ishiguro et al., 2009).

Previous publications (Judák et al., 2014; Maléth et al., 2011 and 2015; Venglovecz et al., 2008) and the present work suggest that etiological factors of AP or pancreatitis itself initiates CFTR mislocalization or degradation, and inhibition of fluid secretion. These factors possibly contribute to increased pancreatic inflammation. We supposed that pharmacological correction of ductal function should reduce pancreatic damage and acinar necrosis/apoptosis of the disease. For this reason, the combination of CFTR corrector, VX-661 and potentiator, VX-770 was used. Pre-treatment of mice with VX-661+VX-770 significantly decreased the pancreatic tissue damage during AP; however, other inflammatory parameters were similar to the AP group. Interestingly, the expression and localization of CFTR protein was not changed by the VX-661 + VX-770 treatment. Since the expression of CFTR was unchanged after VX-661+VX-770 treatments, we suppose that the residual and functional CFTR proteins in pancreatic ducts were activated, and this could lead to the observed decrease in acinar

damage. As localization of CFTR protein was unchanged, we think that the beneficial effect in AP was mainly related to the use of CFTR potentiator (VX-770).

We could demonstrate that CFTR correction and potentiation by VX molecules increases fluid secretion in pancreatic ducts isolated from AP mice. We hypothesize that ductal secretion defends the pancreas by washing out toxic agents like activated digestive enzymes. If this defence mechanism is insufficient, the harmful agents cannot be eliminated from the pancreas, and this can result in tissue damage. Previously, Niderau et al. (1985) and Renner et al. (1983) showed that fluid secretion stimulated by secretin has protective effects in AP. Furthermore, galanin inhibits basal bicarbonate secretion which exacerbates the inflammation of pancreas (Brodish et al., 1994; Hegyi et al., 2011). Overall, it seems that fluid secretion is an important protecting mechanism which can be enhanced in AP by VX-661 + VX-770 treatment.

Zeng et al. (2017) in autoimmune pancreatitis also successfully applied a CFTR corrector (C18) and VX-770, which reduced the extent of inflammation. They observed that increasing CFTR expression (C18) and activity (VX-770), enhanced ductal fluid secretion and clearance of the inflammation to allow repair of cell damage. However, they found that the correction by C18 caused the majority of the effects, and the effect of VX-770 was negligible in that model. In our study, we applied only one AP model, which is a limitation of this work. The secretagogue model utilized in the present investigation damages mainly the pancreatic acinar cells. It would be interesting to test the efficacy of CFTR correction or potentiation in a model where the damage of ducts is likely to initiate the disease. The intraductal taurocholic acid-induced AP model could be used for this reason, which is a well-accepted model of biliary pancreatitis.

Taken together, this study demonstrated CFTR mislocalization and the change of expression during the course of cerulein-induced AP in mice. We also showed that treatment with CFTR correctors and potentiators may offer new option to treat this disease.

References

Ahner A, Gong X and Frizzell RA (2013). Cystic fibrosis transmembrane conductance regulator degradation: cross-talk between the ubiquitylation and SUMOylation pathways. FEBS J 280, 4430-4438.

Amaral MD (2021). How to determine the mechanism of action of CFTR modulator compounds: A gateway to theranostics. Eur J Med Chem 210, 112989.

Abu-El-Haija M, Gukovskaya AS, Andersen DK, Gardner TB, Hegyi P, Pandol SJ, Papachristou GI, Saluja AK, Singh VK, Uc A, Wu BU (2018). Accelerating the Drug Delivery Pipeline for Acute and Chronic Pancreatitis: Summary of the Working Group on Drug Development and Trials in Acute Pancreatitis at the National Institute of Diabetes and Digestive and Kidney Diseases Workshop. Pancreas 47, 1185-1192.

Antigny F, Norez C, Becq F, Vandebrouck C (2008). Calcium homeostasis is abnormal in cystic fibrosis airway epithelial cells but is normalized after rescue of F508del-CFTR. Cell Calcium 43, 175-183.

Argent BE, Arkle S, Cullen MJ, Green R (1986). Morphological, biochemical and secretory studies on rat pancreatic ducts maintained in tissue culture. Q J Exp Physiol 71, 633-648.

Barreto SG, Habtezion A, Gukovskaya A, Lugea A, Jeon C, Yadav D, Hegyi P, Venglovecz V, Sutton R, Pandol SJ (2021). Critical thresholds: key to unlocking the door to the prevention and specific treatments for acute pancreatitis. Gut 70, 194-203.

Banks PA, Bollen TL, Dervenis C, Gooszen HG, Johnson CD, Sarr MG, Tsiotos GG, Vege SS; Acute Pancreatitis Classification Working Group (2013). Classification of acute pancreatitis--2012: revision of the Atlanta classification and definitions by international consensus. Gut 62, 102-111.

Brodish RJ, Kuvshinoff BW, Fink AS, McFadden DW (1994). Inhibition of pancreatic exocrine secretion by galanin. Pancreas9,297-303.

Burghardt B, Elkaer ML, Kwon TH, Rácz GZ, Varga G, Steward MC, Nielsen S (2003). Distribution of aquaporin water channels AQP1 and AQP5 in the ductal system of the human pancreas. Gut 52, 1008-1016.

Crockett SD, Wani S, Gardner TB, Falck-Ytter Y, Barkun AN; American Gastroenterological Association Institute Clinical Guidelines Committee (2018). American Gastroenterological Association Institute Guideline on Initial Management of Acute Pancreatitis. Gastroenterology 154, 1096-1101.

Czakó L, Hegyi P, Rakonczay Z Jr, Wittmann T, Otsuki M (2009). Interactions between the endocrine and exocrine pancreas and their clinical relevance. Pancreatology 9, 351-359.

Fernández-Salazar MP, Pascua P, Calvo JJ, López MA, Case RM, Steward MC, San Román JI (2004). Basolateral anion transport mechanisms underlying fluid secretion by mouse, rat and guinea-pig pancreatic ducts. J Physiol 556, 415-428.

Forsmark CE, Vege SS, Wilcox CM (2016). Acute Pancreatitis. N Engl J Med 375, 1972-1981.

Hegyi P, Venglovecz V, Pallagi P, Maléth J, Takács T, Rakonczay Z Jr (2011). Galanin, a potent inhibitor of pancreatic bicarbonate secretion, is involved in the induction and progression of cerulein-induced experimental acute pancreatitis. Pancreas 40, 155-156.

Hegyi P, Rakonczay Z Jr (2015). The role of pancreatic ducts in the pathogenesis of acute pancreatitis. Pancreatology 15, S13-17.

Hegyi P, Wilschanski M, Muallem S, Lukacs GL, Sahin-Tóth M, Uc A, Gray MA, Rakonczay Z Jr, Maléth J (2016). CFTR: A New Horizon in the Pathomechanism and Treatment of Pancreatitis. Rev Physiol Biochem Pharmacol 170, 37-66.

Ishiguro H, Steward MC, Naruse S, Ko SB, Goto H, Case RM, Kondo T, Yamamoto A (2009). CFTR functions as a bicarbonate channel in pancreatic duct cells. J Gen Physiol 133, 315-326.

Judák L, Hegyi P, Rakonczay Z Jr, Maléth J, Gray MA, Venglovecz V (2014). Ethanol and its non-oxidative metabolites profoundly inhibit CFTR function in pancreatic epithelial cells which is prevented by ATP supplementation. Pflugers Arch 466, 549-562.

Kim Y, Jun I, Shin DH, Yoon JG, Piao H, Jung J, Park HW, Cheng MH, Bahar I, Whitcomb DC, Lee MG (2020). Regulation of CFTR Bicarbonate Channel Activity by WNK1: Implications for Pancreatitis and CFTR-Related Disorders. Cell Mol Gastroenterol Hepatol 9, 79-103.

Kuebler WM, Abels C, Schuerer L, Goetz AE (1996). Measurement of neutrophil content in brain and lung tissue by a modified myeloperoxidase assay. Int J Microcirc Clin Exp 16, 89-97.

Kui B, Balla Z, Vasas B, Végh ET, Pallagi P, Kormányos ES, Venglovecz V, Iványi B, Takács T, Hegyi P, Rakonczay Z Jr (2015). New insights into the methodology of L-arginine-induced acute pancreatitis. PLoS One 10, e0117588.

Li S, Tian B (2017). Acute pancreatitis in patients with pancreatic cancer: Timing of surgery and survival duration. Medicine (Baltimore) 96, e5908.

Lowry OH, Rosebrough NJ, Farr AL, Randall RJ (1951). Protein measurement with the Folin phenol reagent. J Biol Chem 193, 265-275.

Madácsy T, Pallagi P, Maleth J (2018). Cystic Fibrosis of the Pancreas: The Role of CFTR Channel in the Regulation of Intracellular Ca2+ Signaling and Mitochondrial Function in the Exocrine Pancreas. Front Physiol 9, 1585.

Maléth J, Balázs A, Pallagi P, Balla Z, Kui B, Katona M, Judák L, Németh I, Kemény LV, Rakonczay Z Jr, Venglovecz V, Földesi I, Pető Z, Somorácz Á, Borka K, Perdomo D, Lukacs GL, Gray MA, Monterisi S, Zaccolo M, Sendler M, Mayerle J, Kühn JP, Lerch MM, Sahin-Tóth M, Hegyi P (2015). Alcohol disrupts levels and function of the cystic fibrosis transmembrane conductance regulator to promote development of pancreatitis. Gastroenterology 148, 427-439.

Maléth J, Venglovecz V, Rázga Z, Tiszlavicz L, Rakonczay Z Jr, Hegyi P (2011). Non-conjugated chenodeoxycholate induces severe mitochondrial damage and inhibits bicarbonate transport in pancreatic duct cells. Gut 60, 136-138.

Marino CR, Matovcik LM, Gorelick FS, Cohn JA (1991). Localization of the cystic fibrosis transmembrane conductance regulator in pancreas. J Clin Invest 88, 712-716.

Molnár R, Madácsy T, Varga Á, Németh M, Katona X, Görög M, Molnár B, Fanczal J, Rakonczay Z Jr, Hegyi P, Pallagi P, Maléth J (2020). Mouse pancreatic ductal organoid culture as a relevant model to study exocrine pancreatic ion secretion. Lab Invest 100, 84-97.

Niederau C, Ferrell LD, Grendell JH (1985). Caerulein-induced acute necrotizing pancreatitis in mice: protective effects of proglumide, benzotript, and secretin. Gastroenterology 88, 1192-1204.

Mujica VR, Barkin JS, Go VL (2000). Acute pancreatitis secondary to pancreatic carcinoma. Study Group Participants. Pancreas 21, 329-332.

Ooi CY, Dorfman R, Cipolli M, Gonska T, Castellani C, Keenan K, Freedman SD, Zielenski J, Berthiaume Y, Corey M, Schibli S, Tullis E, Durie PR (2011). Type of CFTR mutation determines risk of pancreatitis in patients with cystic fibrosis. Gastroenterology 140, 153-161.

Pallagi P, Balla Z, Singh AK, Dósa S, Iványi B, Kukor Z, Tóth A, Riederer B, Liu Y, Engelhardt R, Jármay K, Szabó A, Janovszky A, Perides G, Venglovecz V, Maléth J, Wittmann T, Takács T, Gray MA, Gácser A, Hegyi P, Seidler U, Rakonczay Z Jr (2014). The role of pancreatic ductal secretion in protection against acute pancreatitis in mice*. Crit Care Med 42, e177-188.

Pallagi P, Hegyi P, Rakonczay Z Jr (2015). The Physiology and Pathophysiology of Pancreatic Ductal Secretion: The Background for Clinicians. Pancreas 44, 1211-1233.

Pallagi P, Madácsy T, Varga Á, Maléth J (2020). Intracellular Ca_2^+ Signalling in the Pathogenesis of Acute Pancreatitis: Recent Advances and Translational Perspectives. Int J Mol Sci 21, 4005.

Pallagi P, Venglovecz V, Rakonczay Z Jr, Borka K, Korompay A, Ozsvári B, Judák L, Sahin-Tóth M, Geisz A, Schnúr A, Maléth J, Takács T, Gray MA, Argent BE, Mayerle J, Lerch MM, Wittmann T, Hegyi P (2011). Trypsin reduces pancreatic ductal bicarbonate secretion by inhibiting CFTR Cl^- channels and luminal anion exchangers. Gastroenterology 141, 2228-2239.

Párniczky A, Kui B, Szentesi A, Balázs A, Szűcs Á, Mosztbacher D, Czimmer J, Sarlós P, Bajor J, Gódi S, Vincze Á, Illés A, Szabó I, Pár G, Takács T, Czakó L, Szepes Z, Rakonczay Z, Izbéki F, Gervain J, Halász A, Novák J, Crai S, Hritz I, Góg C, Sümegi J, Golovics P, Varga M, Bod B, Hamvas J, Varga-Müller M, Papp Z, Sahin-Tóth M, Hegyi P; Hungarian Pancreatic Study Group (2016). Prospective, Multicentre, Nationwide Clinical Data from 600 Cases of Acute Pancreatitis. PLoS One 11, e0165309.

Peery AF, Crockett SD, Barritt AS, Dellon ES, Eluri S, Gangarosa LM, Jensen ET, Lund JL, Pasricha S, Runge T, Schmidt M, Shaheen NJ, Sandler RS (2015). Burden of Gastrointestinal, Liver, and Pancreatic Diseases in the United States. Gastroenterology 149, 1731-1741.

Philippe R, Antigny F, Buscaglia P, Norez C, Becq F, Frieden M, Mignen O (2015). SERCA and PMCA pumps contribute to the deregulation of Ca2+ homeostasis in human CF epithelial cells. Biochim Biophys Acta 1853, 892-903.

Rakonczay Z Jr, Hegyi P, Hasegawa M, Inoue M, You J, Iida A, Ignáth I, Alton EW, Griesenbach U, Ovári G, Vág J, Da Paula AC, Crawford RM, Varga G, Amaral MD, Mehta A, Lonovics J, Argent BE, Gray MA (2008). CFTR gene transfer to human cystic fibrosis pancreatic duct cells using a Sendai virus vector. J Cell Physiol 214, 442-455.

Renner IG, Wisner JR Jr, Rinderknecht H (1983). Protective effects of exogenous secretin on ceruletide-induced acute pancreatitis in the rat. J Clin Invest.72,1081-1092.

Roberts SE, Akbari A, Thorne K, Atkinson M, Evans PA (2013). The incidence of acute pancreatitis: impact of social deprivation, alcohol consumption, seasonal and demographic factors. Aliment Pharmacol Ther 38, 539-548.

Roberts SE, Morrison-Rees S, John A, Williams JG, Brown TH, Samuel DG (2017). The incidence and aetiology of acute pancreatitis across Europe. Pancreatology 17, 155-165.

Venglovecz V, Rakonczay Z Jr, Ozsvári B, Takács T, Lonovics J, Varró A, Gray MA, Argent BE, Hegyi P (2008). Effects of bile acids on pancreatic ductal bicarbonate secretion in guinea pig. Gut 57, 1102-1112.

Zeng M, Szymczak M, Ahuja M, Zheng C, Yin H, Swaim W, Chiorini JA, Bridges RJ, Muallem S (2017). Restoration of CFTR Activity in Ducts Rescues Acinar Cell Function and Reduces Inflammation in Pancreatic and Salivary Glands of Mice. Gastroenterology 153, 1148-1159.

Additional information

Data availability statement

The data that supports the findings of this study are available in the Statistical Summary document.

Competing interest

The authors have no conflicts of interest to declare.

Author contributions

All experiments were carried out at the Department of Pathophysiology and at the First Department of Medicine, University of Szeged (Szeged, Hungary). ZR and LK had the original idea, initiated the study, obtained funding and supervised the experiments. Most the protocols were designed by GF, LK and ZR. GF, ERB, ZB, ESK, BC, DPK, EMO, AS and LK acquired and analysed the data. PH, JM, PP and VV provided conceptual advice on the experimental protocols (JM: confocal microscopy; PP and VV: fluorescence microscopy). GF, LK and ZR wrote the paper. All authors approved the final version of this manuscript and agree to be accountable for all aspects of the work in ensuring that questions related to the accuracy or integrity of any part of the work are appropriately investigated and resolved. All persons designated as authors qualify for authorship, and all those who qualify for authorship are listed.

Funding: This research was supported by EFOP-3.6.2–16–2017–00006, GINOP-2.3.2-15-2016-00048, János Bólyai Research Grant (BO/00866/20/5), ÚNKP Grant (ÚNKP-20-5 - SZTE-163), NKFIH PD129114 and NKFIH K119938. This research was conducted with the support of the Szeged Scientists Academy under the sponsorship of the Hungarian Ministry of Human Capacities (EMMI:13725-2/2018/INTFIN). The funders did not influence the interpretation of results in any way.

Keywords

acute pancreatitis, CFTR, tezacaftor, VX-661, ivacaftor, VX-770

Legends

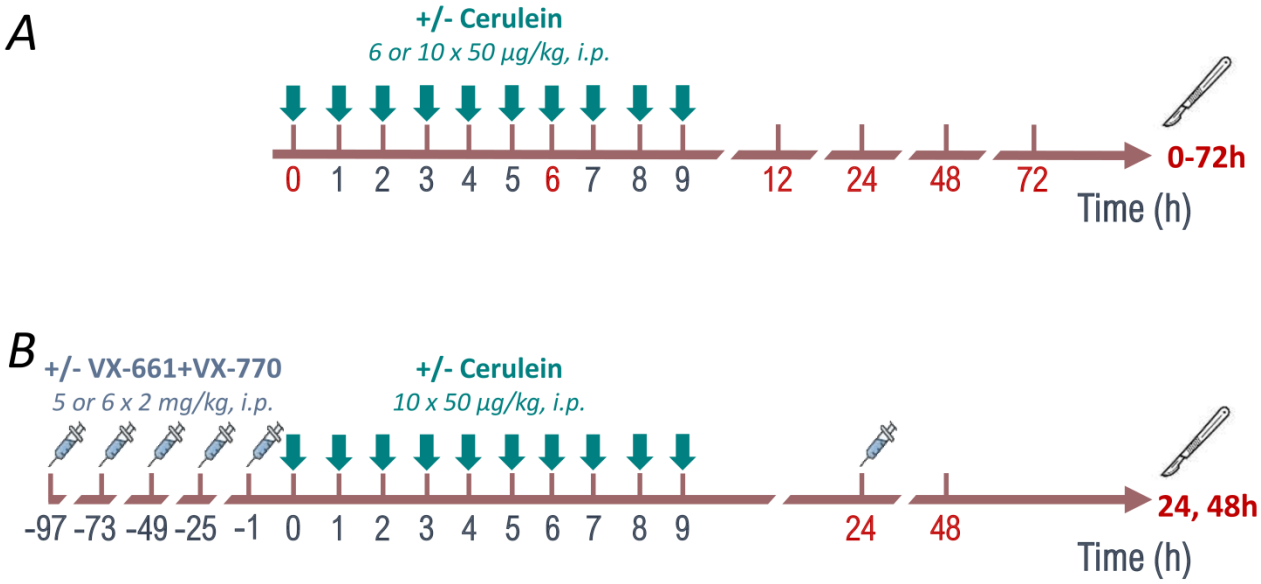

Figure 1. Schematic representation of experimental protocols

Experimental protocol for investigating *A,* the time course of cerulein-induced acute pancreatitis (AP) severity in FVB/n mice; *B*, the effect of CFTR corrector (VX-661) and potentiator (VX-770) on AP. Arrows and syringe pictograms above the timeline indicate cerulein and VX-661/VX-770 treatments, respectively. Control animals were injected with physiological saline (PS) instead of cerulein and DMSO instead of VX compounds. The scalper and red numbers indicate the times of sacrifice in h.

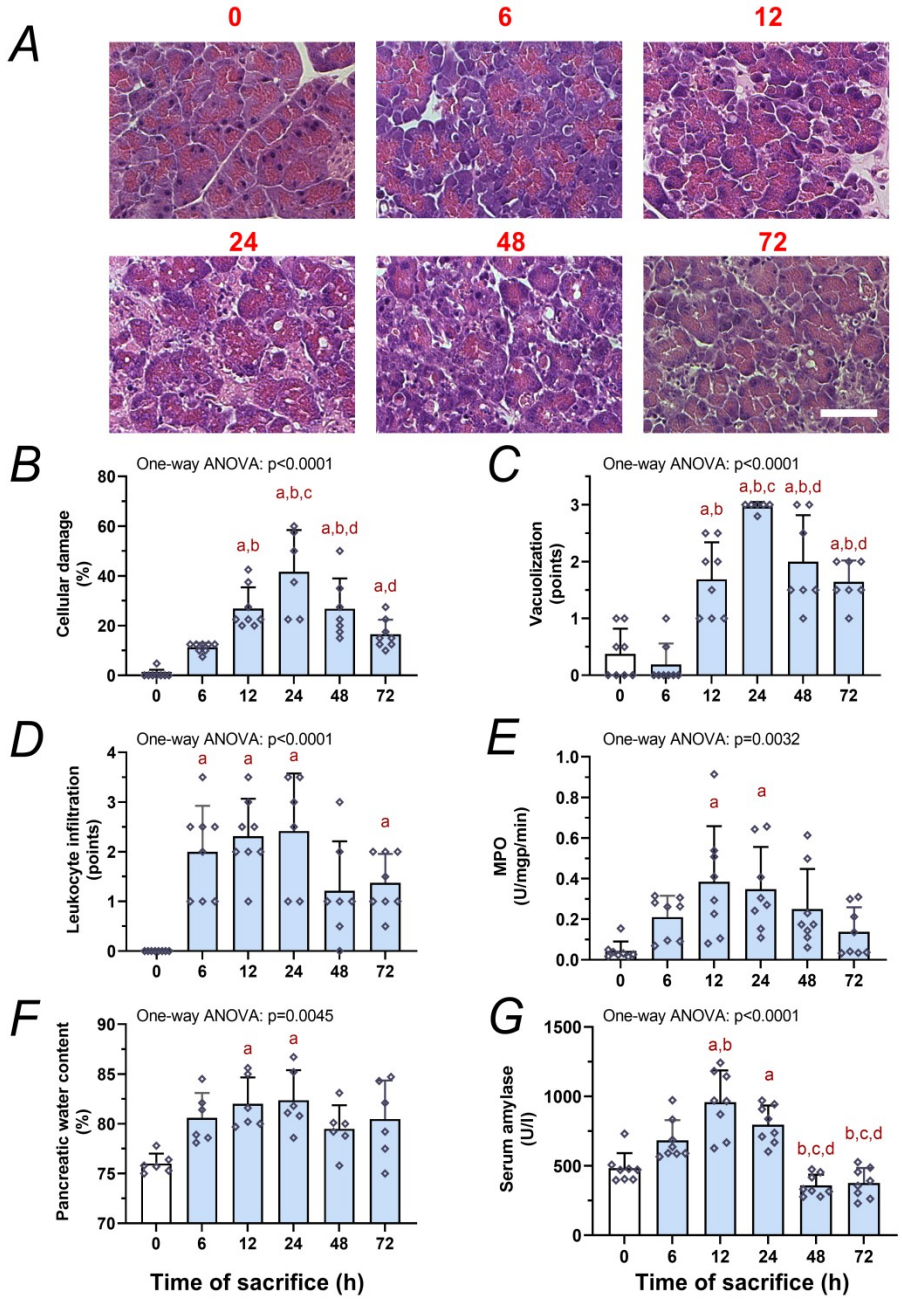

Figure 2. Disease severity course in cerulein-induced acute pancreatitis

A, Representative H&E histopathological images of pancreatic tissues from mice. The groups were established based on time of sacrifice after AP induction (first cerulein injection): 0, 6, 12, 24, 48, 72 hours. Scale bar represents 100 µm. Bar charts show the extent of pancreatic *B*, cellular damage; *C*, vacuolization; *D*, leukocyte infiltration; *E*, myeloperoxidase (MPO) activity; *F*, water content; and *G*, serum amylase activity. Values represent means with standard deviation, n=6-8. One-way ANOVA was performed followed by Tukey HSD post-hoc test. Statistically significant differences ($p<0.05$) were detected and marked with: (a) vs. 0h; (b) vs. 6h; (c) vs. 12h; (d) vs. 24h.

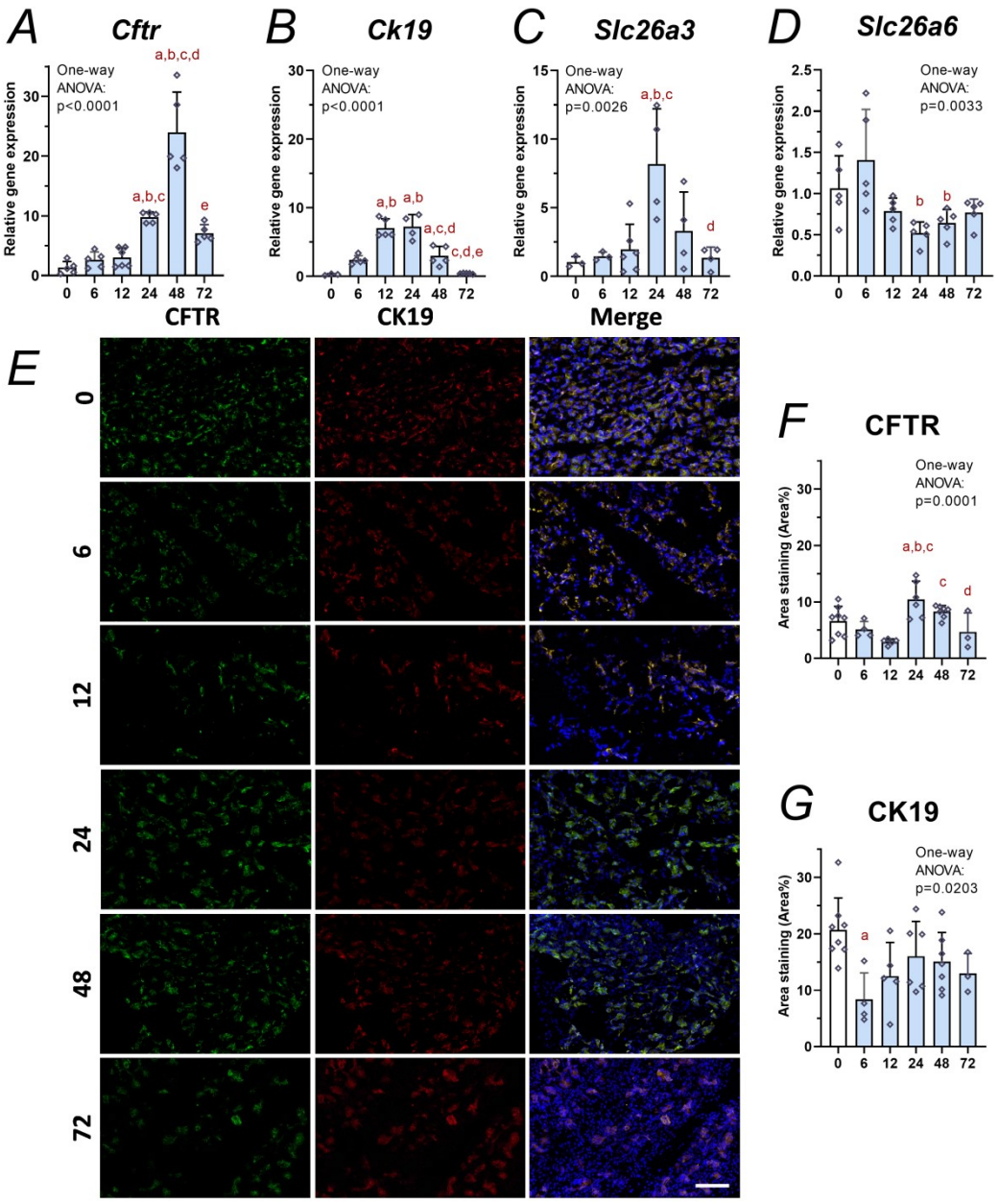

Figure 3. Relative gene expression of *Cftr*, *Ck19*, *Slc26a3*, *Slc26a6* and immunostainings of CFTR and CK19 proteins during the course of acute pancreatitis

Bar charts show the relative gene expression of *A*, *Cftr*; *B*, *Ck19*; *C*, *Slc26a3;* and *D*, *Slc26a6.* Representative immunofluorescent or fluorescent images (CFTR, CK19, and cellular nuclei stainings) of pancreatic tissues from control and Cer-treated animals. Scale bar is 100 µm. Bar charts show the staining area of *F*, CFTR and *G*, CK19 proteins. Values represent means with standard deviation, n=3-7. One-way ANOVA was performed followed by Tukey HSD post-hoc test. Statistically significant differences ($p<0.05$) were detected and marked with: (a) vs. 0h; (b) vs. 6h; (c) vs. 12h; (d) vs. 24h; (e) vs. 48h.

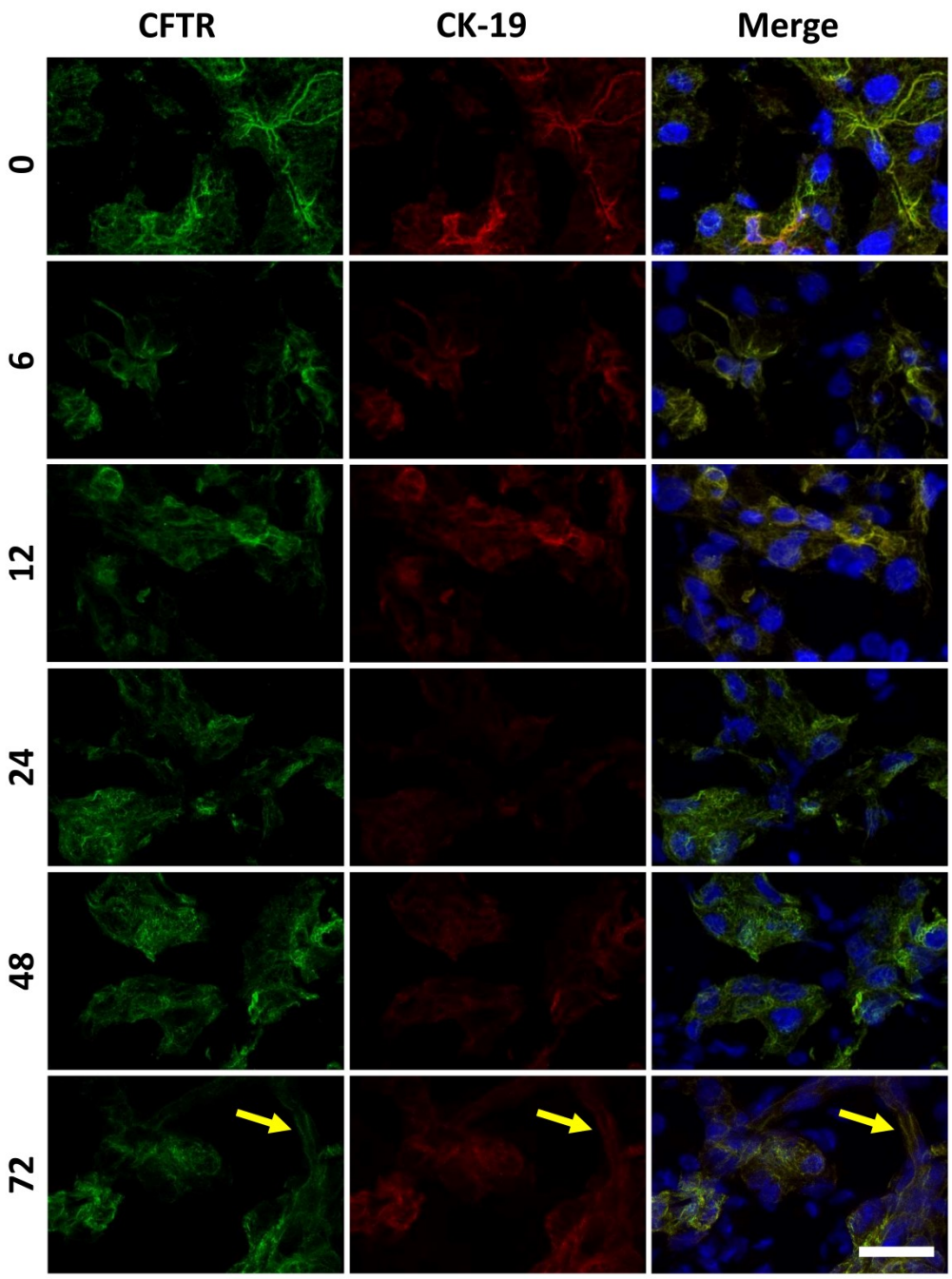

Figure 4. The pancreatic ductal morphology during acute pancreatitis

Fluorescent immunostaining of cystic fibrosis transmembrane conductance regulator (CFTR, green), cytokeratin-19 (CK19, red) proteins and cellular nuclei (blue) in pancreatic tissue of mice with AP observed at 0, 6, 12, 24, 48, 72 h after AP induction. Scale bar = 20 μm.

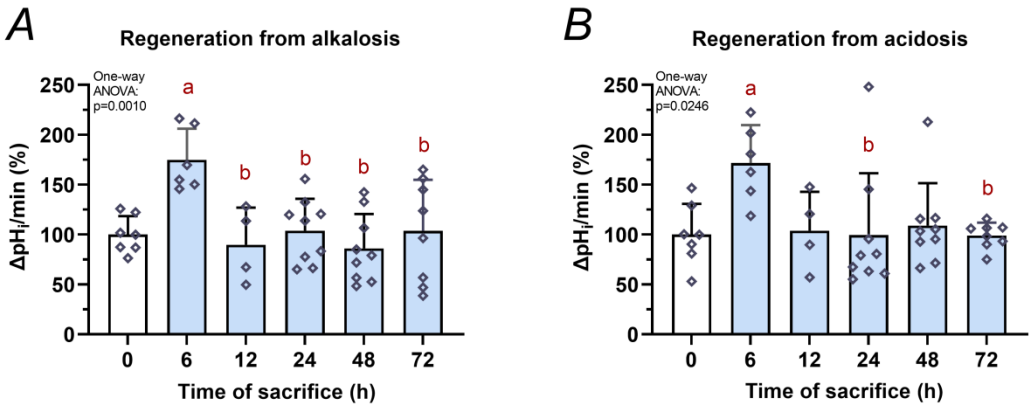

Figure 5. Ductal HCO_3^- secretion during the course of acute pancreatitis

Intra-/interlobular pancreatic ducts were isolated from control (0 h) and AP mice 6-72 h after the first cerulein injection. The measurements of intracellular pH changes (ΔpH_i) are plotted for regeneration from *A,* alkalosis and *B,* acidosis. Values represent means with standard deviation, n=4-9 ducts. One-way ANOVA was performed followed by Tukey HSD post-hoc test. Statistically significant differences ($p<0.05$) were detected and marked with: (a) vs. 0h; (b) vs. 6h.

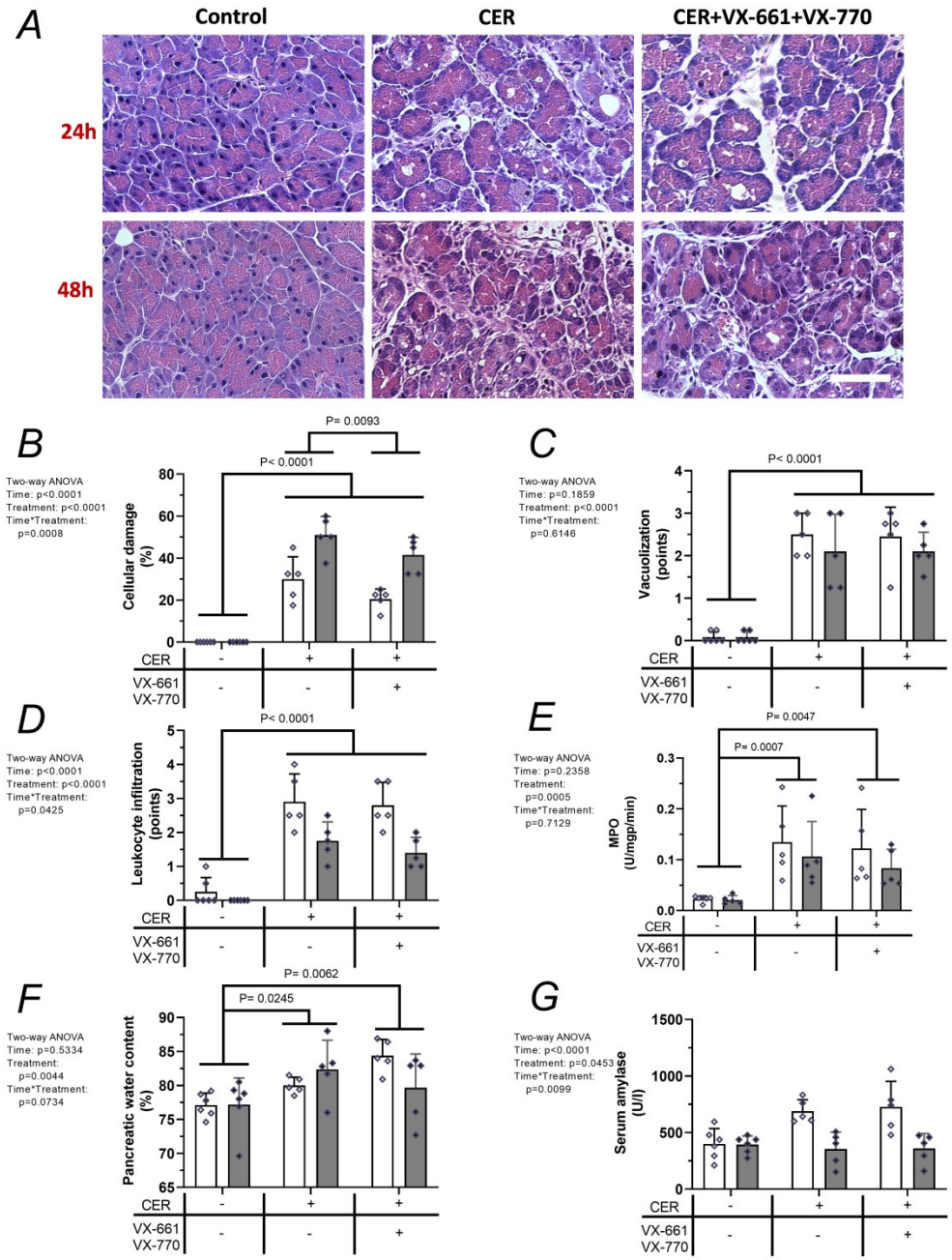

Figure 6. The effect of CFTR corrector VX-661 and CFTR potentiator VX-770 on the severity of acute pancreatitis

A, Representative histopathological images of pancreatic tissues of the treatment groups at 24 or 48 h termination. Bar charts show the extent of pancreatic *B*, cellular damage; *C*, vacuolization; *D*, leukocyte infiltration; *E*, myeloperoxidase (MPO) activity; *F*, water content; and *G*, serum amylase activity measurements. Light and dark grey bars show 24 and 48 h measurements, respectively. Values represent means with standard deviation, n=5-6. Two-way ANOVA was performed followed by Tukey HSD post-hoc test.

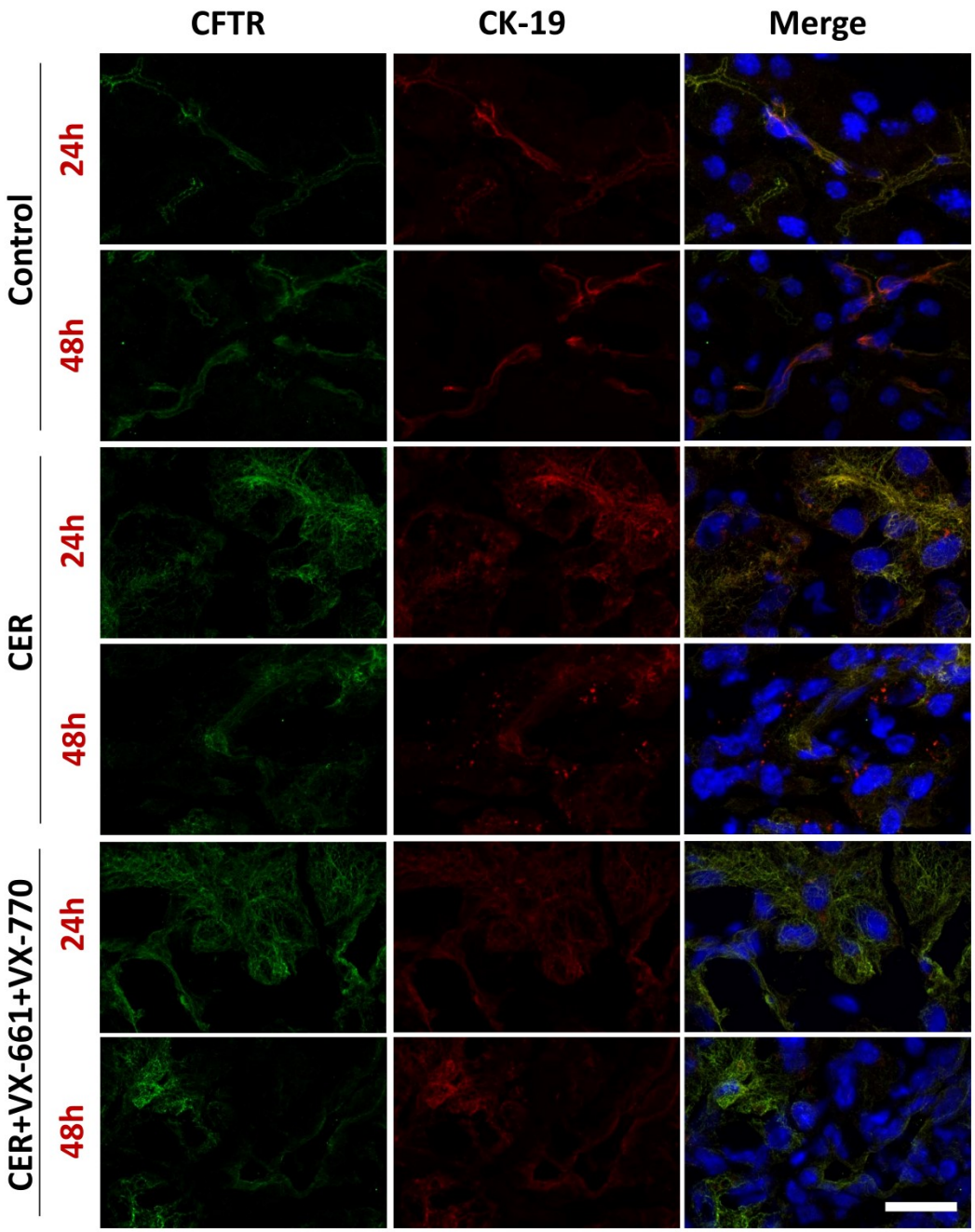

Figure 7. The effect of VX-661 and VX-770 on ductal morphology during acute pancreatitis

Immunofluorescent staining of CFTR (green) and CK19 (red) proteins and cellular nuclei (blue) in pancreatic tissues from mice at 24 or 48 h after AP induction. Treatment groups: control; Cer-induced AP; Cer-induced AP+VX-661+VX-770. Scale bar = 20 μm.

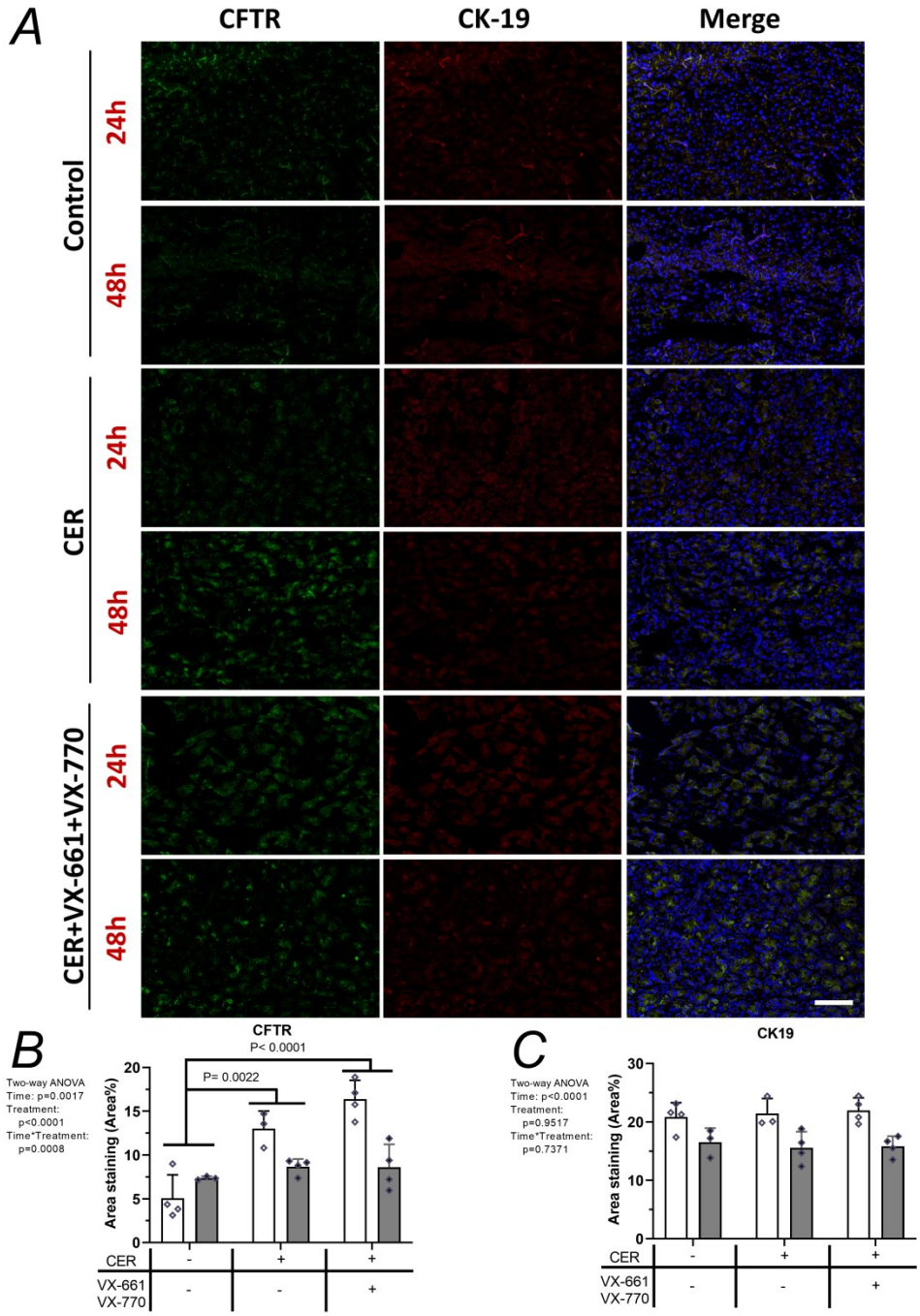

Figure 8. The effect of VX-661 and VX-770 on the protein expression of CFTR and CK19 during acute pancreatitis

A, Representative immunofluorescent images (CFTR, CK19, and cellular nuclei stainings) of pancreatic tissues. Treatment groups: control; Cer-induced AP; Cer-induced AP+VX-661+VX-770. Bar charts show the staining area of *B*, CFTR and *C*, CK19 proteins. Scale bar is 100 µm. Light and dark grey bars show 24 and 48 h measurements, respectively. Values represent means with standard deviation, n=3-5. Two-way ANOVA was performed followed by Tukey HSD post-hoc test.

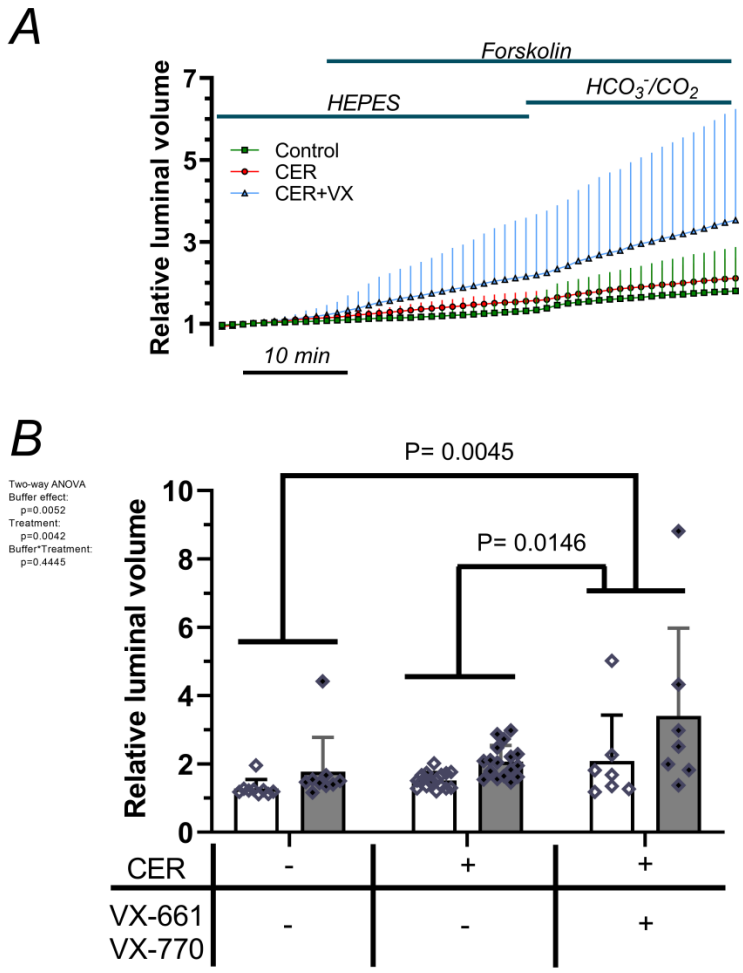

Figure 9. The effect of VX-661 and VX-770 on the fluid secretion of isolated pancreatic ducts

Intra-/interlobular pancreatic ducts were isolated from control and AP mice 6 h after the first cerulein injection. Thereafter, ducts were cultured for 6-14 h (which allowed sealing of their open ends) at 37 °C in a humidified atmosphere containing 5% CO_2. 3 µM VX-661 and 1 µM VX-770 or their vehicle (DMSO) were administered in the culture media of some AP ducts. Since DMSO had no effect on the swelling of ducts isolated from AP mice, the corresponding groups treated with or without DMSO (media) were combined. *A*, the line diagram shows changes in relative luminal volume of pancreatic ducts derived from control and AP mice with or without VX treatment in response to administration of standard HEPES and HCO_3^-/CO_2 containing solutions. Fluid secretion was stimulated with the cAMP agonist forskolin. *B*, Bar charts show the relative luminal volume measured before the end of 'standard HEPES buffer + forskolin' (light bars) and 'standard HCO_3^-/CO_2 buffer + forskolin' (dark bars) perfusion. Values represent means with standard deviation, n=7-17. Two-way ANOVA was performed followed by Tukey HSD post-hoc test.

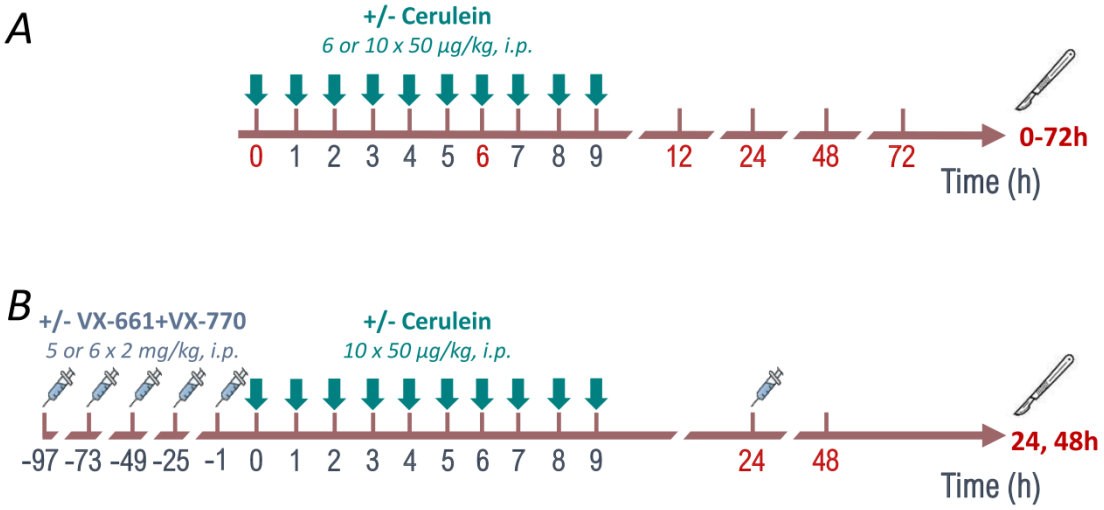

Experimental setups for investigating the time course of cerulein-induced acute pancreatitis (AP) and the effect of CFTR corrector (VX-661) and potentiator (VX-770) on AP.

Gabriella Fűr is a PhD candidate at the University of Szeged, Department of Pathophysiology. Her supervisors are Prof. Dr. Zoltán Rakonczay Jr. and Dr. Lóránd Kiss. Previously, Gabriella received her MSc degree as a Neuroscience and Human biologist from the University of Szeged, Faculty of Science and Informatics in 2016. Currently, her research focuses on acute pancreatitis (AP), mislocalization of CFTR expression and investigation of CFTR correctors and potentiators in AP. Her main goal is to study new drugs in relation to AP. In the future she will continue her research in the field of AP in translational perspectives.